Modeling of the atmospheric boundary layer structure above a thermally nonuniform surface

A.F. Kurbatskii and L.I. Kurbatskaya*

Institute of Theoretical and Applied Mechanics,
Siberian Branch of the Russian Academy of Sciences, Novosibirsk
Novosibirsk State University
** Institute of Computational Mathematics and Mathematical Geophysics,*
Siberian Branch of the Russian Academy of Sciences, Novosibirsk

Received December 14, 2004

Some results on modeled atmospheric boundary layer (ABL) structure above a thermally nonuniform surface (a heat island of limited size) are presented. To calculate the turbulent momentum and heat fluxes, the completely explicit algebraic models have been developed using the symbolic algebra from the transport equations in the approximation of weak-equilibrium turbulence. To provide for closure of the algebraic equations for turbulent fluxes, a three-parameter $E - \varepsilon - \langle\theta^2\rangle$ model of thermally stratified turbulence has been used. A two-dimensional computer test of a 24-hour ABL evolution shows that the third-order closure turbulence model (in Mellor and Yamada terminology) is capable of reconstructing the most important structure features of the ABL above the ground with a heat island, including those, which cannot be reconstructed with the $k - \varepsilon$ turbulence model. The results obtained well agree with the measurements and the numerical results of other authors.

Introduction

The problems of assessing the quality of air in urban areas are complicated because of a wide variety of spatial and temporal scales, within which the corresponding phenomena occur. In particular, two most important scales are the city scale of about several tens of kilometers (typical city scale), at which the primary emission of air pollutants occurs, and the mesoscale of about several hundreds of kilometers, at which secondary air pollutants are formed and spread. Therefore, the spread of pollutants strongly depends on the structure of the urban boundary layer and its interactions with the synoptic current and the surface. This system is characterized by strong nonlinearity, and therefore numerical models are usually used to study the problems of environmental pollution.

To calculate the mean and turbulent transport and chemical transformations of pollutants, it is necessary to know, as accurate as possible, the main meteorological parameters, such as the wind, turbulent momentum, heat, and matter fluxes, temperature, pressure, and humidity, which can be either interpolated from measurements or calculated using mesoscale circulation models (see, for example, Ref. 1).

Ideally, these models should be capable of resolving two main scales: the city scale and the mesoscale. Since the horizontal dimensions of a region are on the order of the mesoscale (100 km), the step of the computational grid, minimized in terms of the needed computation time, ranges generally from several hundreds of meters to several kilometers. This means that it is impossible to resolve the structure of an urban surface in detail and the effects of urban surfaces should be parameterized.

Here we would like to note two most important effects of the urban surface on the structure of the airflows above it (see, for example, Ref. 2):

1. Resistance to the incoming airflow from buildings (different pressures across the roughness elements).

2. Differential heating/cooling of the urban surfaces, which can give rise to the so-called heat island effect.

The latter effect on the ABL structure is considered in this paper in a simplified form for a flat surface with the given roughness. As a thermal boundary condition, we define the surface temperature, modeling the ground heating by the sun in the 24-hour evolution cycle. The effect of the urban heat island is simulated by defining the temperature contrast at a limited part of the surface (the boundary conditions are considered in a more detail below, in Subsection 2.1). This simplified model of the urban heat island is a good test for a mesoscale model of the turbulent atmospheric flow over the thermally nonuniform surface.

1. Mesoscale model of the atmospheric flow over the thermally nonuniform surface

The investigations on the parameterization of turbulence (Reynolds shear stresses) were started in 1940s (Kolmogorov, Ref. 5). The models of turbulent shear stresses were then verified experimentally (using the data of measurements, in particular, by

0235-6880/05/05–06 399-10 $02.00

comparing with the data obtained by large-eddy modeling of turbulence) and applied in various engineering problems. In geophysical approximations, turbulence closure models of different degree of complexity were formulated by Mellor and Yamada[3,4] and used for modeling the planetary boundary layer with a greater success, than many empirical models.

Recently in Ref. 6, the modified 2.5-level closure turbulence model was formulated, in which some simplifications of the 2.5-level model[3,4] were removed owing to the use of most complete Zeman–Lumley model[7] for the correlation of the dynamic Π_{ij} and temperature $\Pi_{i\theta}$ turbulent fields having pressure pulsations. In the 2.5-level turbulence model, all turbulent fluxes of momentum (Reynolds shear stresses) and heat, including the variance of turbulent temperature fluctuations $<\theta^2>$, are calculated from algebraic equations.

In Refs. 8 and 9, somewhat different, but, as in Ref. 7, tensor-invariant models for correlation of Π_{ij} and $\Pi_{i\theta}$ were proposed. These models were used to formulate the three-parameter turbulence model in this paper. As in Ref. 7, the parameterization of Π_{ij} and $\Pi_{i\theta}$ correlations includes the buoyancy effects, while for the "fast" terms the tensor-invariant IP model is used.[9]

The model of the slow part of the correlation has a simple relaxation form: $\Pi_{ij}^{(1)} \sim b_{ij}/\tau$ (where $b_{ij} = <u_iu_j> - (2E/3)\delta_{ij}$ is the anisotropy tensor; $E = <u_iu_j>/2$ is the kinetic energy of turbulence (KET); $\tau = E/\varepsilon$ is the dynamic temporal scale of turbulence; ε is the KET dissipation). In this model, the symmetric S_{ij} and asymmetric Ω_{ij} parts of the mean deformation rate tensor in the "fast" part of the $\Pi_{ij}^{(2)}$ correlation have identical numerical coefficients as in Refs. 8 and 9 and different coefficients in the model from Ref. 6.

The original Mellor–Yamada 2.5-level closure model uses simpler parameterizations for the correlation between the dynamic and temperature fields with the pressure pulsations in the form: $\Pi_{ij}^{(1)} \sim b_{ij}/\tau$, $\Pi_{ij}^{(2)} \sim -ES_{ij}$, $\Pi_{ij}^{(3)} = 0$ (buoyancy contribution); $\Pi_i^{\theta(1)} \sim h_i/\tau_\theta$ (where $h_i = <u_i\theta>$ is the turbulent heat flux vector, τ_θ is the temporal scale of the turbulent temperature field), $\Pi_i^{\theta(2)} = \Pi_i^{\theta(3)} = 0$. Consequently, the Mellor–Yamada model accounts for one fast term ($\Pi_{ij}^{(2)}$) and neglects the buoyancy effects (terms $\Pi_i^{\theta(2)}$ and $\Pi_i^{\theta(3)}$). Thus, the parameterizations of the turbulent momentum and heat fluxes, presented in this paper, occupy an intermediate position between the "structure-symmetric" parameterizations of the modified model[6] and the Mellor–Yamada parameterizations.

The modified 2.5-level closure model was tested in Ref. 6 with the standard problem of a horizontally homogeneous planetary boundary layer. However, even this simple problem under conditions of unstable stratification requires careful calculation of the counter-gradient heat flux in the inversion layer. The algebraic parameterization for the calculation of the temperature variance $<\theta^2>$ (used in the 2.5-level models) appears to be insufficient for this purpose, and it is necessary to solve the transfer equation for the temperature variance in order to adequately take into account the processes of advection, diffusion, and destruction for this parameter. The model of turbulent momentum and heat fluxes for environmental flows is considered in detail in Subsection 1.3.

1.1. Basic equations

To model flows in the atmospheric boundary layer, the equations for the mean and turbulent parameters are needed. The basic equations have the form:

for the mean velocity U_i:

$$\frac{DU_i}{Dt} = -\frac{\partial}{\partial x_j}\tau_{ij} - g_i - \frac{1}{\rho}\frac{\partial P}{\partial x_i} - 2\varepsilon_{ijk}\Omega_j U_k; \quad (1a)$$

for the mean potential temperature Θ:

$$\frac{D\Theta}{Dt} = -\frac{\partial}{\partial x_j}h_j, \quad (1b)$$

where

$$\frac{D}{Dt} \equiv \frac{\partial}{\partial t} + U_j\frac{\partial}{\partial x_j}; \quad \tau_{ij} \equiv <u_iu_j>; \quad h_i \equiv <u_i\theta>. \quad (1c)$$

Here u_i is the component of turbulent velocity fluctuations; $g_i = (0,0,g)$ is the acceleration due to gravity; P is the mean pressure; ρ is the mean density; Ω_j is the vector of the angular rate of the Earth rotation; τ_{ij} are the Reynolds shear stresses, and h_j is the vector of the turbulent heat flux.

For flows in the planetary boundary layer, some approximations can be accepted in the basic equations. In Eq. (1a), the rotation term can be approximated as

$$-2\varepsilon_{ijk}\Omega_j U_k = f_c\varepsilon_{ij3}U_j, \quad (1d)$$

where the axes x, y, and z are directed to the east, north, and vertically, respectively; $f_c = 2\Omega\sin\phi$ is the Coriolis parameter with the angular rate of the Earth rotation Ω and the latitude ϕ. The buoyancy effects are taken into account in the Boussinesq approximation, and for the two-dimensional, on the average, flow the system of equations (1a)–(1b) can be written in the form

$$U_x + W_z = 0, \quad (1e)$$

$$U_t + UU_x + WU_z = -\frac{1}{\rho}P_x - <wu>_z + fV; \quad (1f)$$

$$V_t + UV_x + WV_z = -<wv>_z - fU; \quad (1g)$$

$$W_t + UW_x + WW_z = -\frac{1}{\rho_0}P_z - <ww>_z + \beta\Theta g; \quad (1h)$$

$$\Theta_t + U\Theta_x + W\Theta_z = -<u\theta>_x - <w\theta>_z. \quad (1i)$$

The dependent variables in Eqs. (1a)–(1i) are the Reynolds (i.e., time-averaged) velocities U, V, and W along the x, y, and z axes, respectively; Θ is the

mean deviation of the potential temperature from the standard value T_0; β is the volume expansion coefficient of the air ($3.53 \cdot 10^{-3}$ K^{-1}); ρ_0 is the mean air density, lower-case characters denote turbulent fluctuations of the corresponding parameters. Turbulent (Reynolds) shear stresses τ_{ij} and the turbulent heat flux vector h_j in the system of equations (1d)–(1i) call for modeling. The completely explicit algebraic models for the Reynolds shear stresses and the turbulent heat flux are formulated in the following two subsections.

1.2. Turbulence equations

1) Equations for the Reynolds shear stresses τ_{ij}:

$$\frac{D}{Dt}\tau_{ij} + D_{ij} = -\left(\tau_{ik}\frac{\partial U_j}{\partial x_k} + \tau_{jk}\frac{\partial U_i}{\partial x_k}\right) + \\ + \beta_i h_j + \beta_j h_i - \Pi_{ij} - \varepsilon_{ij}, \quad (2a)$$

where

$$\Pi_{ij} \equiv < u_i \frac{\partial p}{\partial x_j} > + < u_j \frac{\partial p}{\partial x_i} > - \frac{2}{3}\delta_{ij} < p u_k >; \quad (2b)$$

$$\varepsilon_{ij} \equiv 2\nu < \frac{\partial u_i}{\partial x_k}\frac{\partial u_j}{\partial x_k} > = \frac{2}{3}\delta_{ij}\varepsilon; \quad \beta_i \equiv \beta g_i; \quad (2c)$$

$$D_{ij} \equiv \frac{\partial}{\partial x_k}\left(< u_i u_j u_k > + \frac{2}{3}\delta_{ij} < p u_k >\right). \quad (2d)$$

Here Π_{ij} is the tensor of the pressure–velocity correlation; p is the turbulent fluctuation of pressure; ν is the molecular viscosity coefficient; D_{ij} is the diffusion term.

2) The balance equation for the kinetic energy of turbulence (KET) E:

$$\frac{DE}{Dt} + \frac{1}{2}D_{ii} = -\tau_{ij}\frac{\partial U_i}{\partial x_j} + \beta_i h_i - \varepsilon. \quad (2e)$$

3) The transfer equation for the turbulent heat flux h_i:

$$\frac{D}{Dt}h_i + D_i^h = -h_j\frac{\partial U_i}{\partial x_j} - \tau_{ij}\frac{\partial \Theta}{\partial x_j} + \beta_i < \theta^2 > - \Pi_i^\theta, \quad (3a)$$

where

$$\Pi_i^\theta \equiv < \theta \frac{\partial p}{\partial x_i} >; \quad D_i^h = \frac{\partial}{\partial x_j} < u_i u_j \theta >; \quad (3b)$$

Π_i^θ is the pressure–temperature correlation; D_i^h is the diffusion of the heat flux h_i.

4) The transfer equation for the temperature variance $<\theta^2>$:

$$\frac{D}{Dt} < \theta^2 > + D_\theta = -2h_i\frac{\partial \Theta}{\partial x_i} - 2\varepsilon_\theta, \quad (4a)$$

where

$$\varepsilon_\theta \equiv \chi < \left(\frac{\partial \theta}{\partial x_j}\right)^2 >; \quad D_\theta = \frac{\partial}{\partial x_i} < u_i \theta^2 >; \quad (4b)$$

χ is the molecular thermal diffusivity; D_θ is the diffusion of temperature variance; ε_θ is the dissipation rate of temperature variance.

5) The equation of spectral consumption of KET (its dissipation rate) ε:

$$\frac{D\varepsilon}{Dt} + D_\varepsilon = -\frac{\varepsilon}{\tau}\Psi, \quad (5a)$$

where

$$\Psi = \psi_0 + \psi_1\frac{b_{ij}}{\varepsilon}\frac{\partial U_i}{\partial x_j} + \psi_2\frac{\beta_i}{\varepsilon} < \theta u_i > + \\ + \psi_3\beta_j\frac{2E}{\varepsilon} < \theta u_i > \frac{\partial U_i}{\partial x_j}; \quad (5b)$$

$$D_\varepsilon = \frac{\partial}{\partial x_j} < \varepsilon u_j >; \quad (5c)$$

ψ_0, ψ_1, and ψ_2 are numerical coefficients (determined in Subsection 1.3).

In this study, the terms including the molecular viscosity ν and the molecular thermal diffusivity χ are neglected, except for the equations for ε_{ij} and ε_θ. In addition, the rotation is neglected in the equations for second moments. The modeling of third-order moments is beyond the scope of this work. As was already mentioned, the main task of this study is to obtain the parameterizations of turbulent heat and momentum fluxes in the approximation of weak-equilibrium turbulence,[10] with the use of which the modeling of the third-order moments is not necessary.

1.3. Third-order closure turbulence model

1.3.1. Model for correlation with pressure pulsations

The correlations with pressure pulsations Π_{ij} and Π_i^θ in Eqs. (2a) and (3a) include three different contributions caused by: 1) self-actions of the turbulence field (tendency to isotropy or "slow" part of correlation), 2) interactions between the mean velocity shear and turbulence ("fast" part of correlation), and 3) interactions between buoyancy and turbulence ("fast" part as well):

$$\Pi_{ij} = \Pi_{ij}^{(1)} + \Pi_{ij}^{(2)} + \Pi_{ij}^{(3)}, \\ \Pi_i^\theta = \Pi_i^{\theta(1)} + \Pi_i^{\theta(2)} + \Pi_i^{\theta(3)}, \quad (6a)$$

where

$$\Pi_{ij}^{(1)} = c_1\tau^{-1}b_{ij},$$

$$\Pi_{ij}^{(2)} = -\frac{4}{3}c_2 E S_{ij} - c_2\left(Z_{ij} + \Sigma_{ij}\right), \quad \Pi_{ij}^{(3)} = c_3 B_{ij},$$

$$\Pi_i^{\theta(1)} = c_{1\theta}\tau^{-1}h_i, \quad \Pi_i^{\theta(2)} = -c_{2\theta}h_j\frac{\partial U_i}{\partial x_j},$$

$$\Pi_i^{\theta(3)} = c_{3\theta}\beta_i < \theta^2 >; \quad (6b)$$

$$S_{ij} = \frac{1}{2}\left(\frac{\partial U_i}{\partial x_j} + \frac{\partial U_j}{\partial x_i}\right); \quad R_{ij} = \frac{1}{2}\left(\frac{\partial U_i}{\partial x_j} - \frac{\partial U_j}{\partial x_i}\right); \quad (6c)$$

$$\Sigma_{ij} = b_{ik}S_{kj} + S_{ik}b_{kj} - \frac{2}{3}\delta_{ij}b_{km}S_{mk};$$

$$Z_{ij} = R_{ik}b_{kj} - b_{ik}R_{kj};$$

$$B_{ij} = b_i h_j + b_j h_i - \frac{2}{3}\delta_{ij}b_k h_k\,, \qquad (6d)$$

S_{ij} and R_{ij} are the tensors of the mean shear and the mean vorticity, respectively. As was already mentioned above, for the "fast" part of correlation $\Pi_{ij}^{(2)}$ the tensor-invariant IP-model, developed by Launder,[8,9] is used.

1.3.2. Algebraic models of the Reynolds shear stresses and the heat flux vector

The combination of Eqs. (2a) and (2e) allows us to write the equation for the anisotropy tensor b_{ij}:

$$\frac{D}{Dt}b_{ij} + D_{ij} = -\frac{4}{3}ES_{ij} - \Sigma_{ij} - Z_{ij} + B_{ij} - \Pi_{ij}. \quad (7a)$$

Equation (7a) can be simplified in the approximation of the weak-equilibrium turbulence, which states that the turbulence is in the equilibrium with the imposed mean parameters. The equilibrium state of turbulence can be obtained, if we take that the substantial derivative of the anisotropy tensor is zero. Then, in the approximation of the weak-equilibrium turbulence, it is assumed that the turbulent transfer of the anisotropy tensor D_{ij} is negligibly small and, once Eq. (6b) for the pressure–velocity correlation Π_{ij} is substituted in the right-hand side of Eq. (7a), we obtain the algebraic equation for the tensor b_{ij}:

$$b_{ij} = -\alpha_1 E\tau S_{ij} - \alpha_2\tau\left(\Sigma_{ij} + Z_{ij}\right) + \alpha_3\tau B_{ij}, \qquad (8a)$$

where

$$\alpha_1 = \frac{4}{3}\frac{1-c_2}{c_1}\,,\ \alpha_2 = \frac{1-c_2}{c_1}\,,\ \alpha_3 = \frac{1-c_3}{c_1}\,. \qquad (8b)$$

The constants of the model c_1, c_2, and c_3 are determined in Subsection 1.4.

Applying the equation of the weak-equilibrium turbulence to the prognostic equation (3a) along with Eq. (6b) for the correlation Π_i^θ, we obtain the algebraic equation for the heat flux vector h_i (third-order closure model in the Mellor–Yamada classification):

$$A_{ij}h_j = -\tau\left(b_{ij} + \frac{2}{3}E\delta_{ij}\right)\frac{\partial\Theta}{\partial x_j} + \tau\alpha_4\beta g\delta_{i3} < \theta^2>, \qquad (9a)$$

where

$$A_{ij} = \alpha_5\delta_{ij} + \tau\alpha_4\frac{\partial U_i}{\partial x_j}; \qquad (9b)$$

$$\alpha_4 = (1 - c_{2\theta})\,,\ \alpha_5 = \frac{c_{1\theta}}{\sqrt{2R}} \qquad (9c)$$

(R is defined below in Eq. (12b)).

Note that for the thermally stratified third-order closure turbulence the variance of temperature fluctuations $<\theta^2>$ is not parameterized, but is determined from the prognostic differential transfer equation (4a). Thus, the algebraic equations for the turbulent heat and momentum fluxes take the closed form when using the three-parameter $E - \varepsilon - <\theta^2>$-model of turbulence.

In the boundary-layer approximation, from the algebraic equations (8a) and (9a) for the turbulent fluxes $<u_iu_j>$ and $<u_i\theta>$, we can write a system of implicit equations for the turbulent momentum and heat fluxes:

$$< u^2 >= \frac{2}{3}E - \frac{\tau}{3}\left(4\alpha_2\frac{\partial U}{\partial z} <uw> - \right.$$

$$\left. -2\alpha_2\frac{\partial V}{\partial z} <vw> + 2\alpha_3\beta g <w\theta>\right); \qquad (10a)$$

$$<v^2>= \frac{2}{3}E - \frac{\tau}{3}\left(4\alpha_2\frac{\partial V}{\partial z} <vw> - \right.$$

$$\left. -2\alpha_2\frac{\partial U}{\partial z} <uw> + 2\alpha_3\beta g <w\theta>\right); \qquad (10b)$$

$$<w^2>= \frac{2}{3}E + \frac{\tau}{3}\left(2\alpha_2\frac{\partial U}{\partial z} <uw> + \right.$$

$$\left. +2\alpha_2\frac{\partial V}{\partial z} <vw> + 4\alpha_3\beta g <w\theta>\right); \qquad (10c)$$

$$<uw>= -\frac{\tau}{2}\frac{\partial U}{\partial z}2\alpha_2 <w^2> + \alpha_3\tau\beta g <u\theta>; \quad (10d)$$

$$<vw>= -\frac{\tau}{2}\frac{\partial V}{\partial z}2\alpha_2 <w^2> + \alpha_3\tau\beta g <v\theta>; \quad (10e)$$

$$<uv>= -\tau\alpha_2\left(\frac{\partial V}{\partial z} <uw> + \frac{\partial U}{\partial z} <vw>\right); \quad (10f)$$

$$<u\theta>= -\frac{\tau}{\alpha_5}\left(\frac{\partial\Theta}{\partial z} <uw> + \alpha_4\frac{\partial U}{\partial z} <w\theta>\right); \quad (10g)$$

$$<v\theta>= -\frac{\tau}{\alpha_5}\left(\frac{\partial\Theta}{\partial z} <vw> + \alpha_4\frac{\partial V}{\partial z} <w\theta>\right); \quad (10h)$$

$$<w\theta>= -\frac{\tau}{\alpha_5}\left(\frac{\partial\Theta}{\partial z} <w^2> - \alpha_4\beta g <\theta^2>\right). \quad (10i)$$

Equations (10a)–(10i) were solved using symbolic algebra. Below we present the equations for those turbulent momenta and heat fluxes, which are used in the numerical tests for solution of the system of equations (1e) – (1i):

$$\left(<uw>, <vw>\right) = -K_M\left(\frac{\partial U}{\partial z}, \frac{\partial V}{\partial z}\right); \qquad (11a)$$

$$<w\theta>= -K_H\frac{\partial\Theta}{\partial z} + \gamma_c; \qquad (11b)$$

$$K_M = E\tau S_M,\ K_H = E\tau S_H; \qquad (11c)$$

$$S_M = \frac{1}{D}\left\{s_0\left[1 + s_1 G_H (s_2 - s_3 G_H)\right] + \right.$$

$$\left. + s_4 s_5 (1 + s_6 G_H)\tau\beta g \frac{<\theta^2>}{E}\right\}, \quad (11d)$$

$$S_H = \frac{1}{D}\left\{\frac{2}{3}\frac{1}{\alpha_5}(1 + s_6 G_H)\right\}, \quad (11e)$$

where

$$\gamma_c = \frac{1}{D}\left\{1 + \frac{2}{3}\alpha_2^2 G_M + s_6 G_H\right\}\alpha_6(\tau\beta g) <\theta^2> \quad (11f)$$

is the counter-gradient term, which is absent in the 2- and 2.5-order closure models.[3,4,6]

The parameters G_H and G_M are determined as

$$G_H \equiv (\tau N)^2, \quad G_M \equiv (\tau S)^2; \quad (11g)$$

$$N^2 = \beta g \frac{\partial \Theta}{\partial z}, \quad S^2 \equiv \left(\frac{\partial U}{\partial z}\right)^2 + \left(\frac{\partial V}{\partial z}\right)^2; \quad (11h)$$

$$D = 1 + d_1 G_M + d_2 G_H + d_3 G_M G_H + d_4 G_H^2 + $$
$$+\left[d_5 G_H^2 - d_6 G_M G_H\right] G_H; \quad (11i)$$

$$d_1 = \frac{2}{3}\alpha_2^2, \quad s_0 = \frac{2}{3}\alpha_2,$$

$$d_2 = \frac{10}{3}\frac{\alpha_3}{\alpha_5}, \quad s_1 = \frac{1}{\alpha_2}\left(\frac{\alpha_3}{\alpha_5}\right),$$

$$d_3 = \frac{2}{3}\alpha_2\frac{\alpha_3}{\alpha_5}(\alpha_2 - \alpha_6); \quad s_2 = \alpha_2 - \alpha_6,$$

$$d_4 = \frac{11}{3}\left(\frac{\alpha_3}{\alpha_5}\right)^2, \quad s_3 = \alpha_6\left(\frac{\alpha_3}{\alpha_5}\right),$$

$$d_5 = \frac{4}{3}\left(\frac{\alpha_3}{\alpha_5}\right)^3, \quad s_4 = \alpha_3\alpha_6,$$

$$d_6 = \frac{2}{3}\alpha_2\alpha_6\left(\frac{\alpha_3}{\alpha_5}\right)^2, \quad s_5 = \alpha_6 + \frac{4}{3}\alpha_2,$$

$$s_6 = \frac{\alpha_3}{\alpha_5}; \quad \alpha_6 = \frac{1 - C_{2\theta}}{C_{1\theta}}. \quad (11j)$$

The variance of the vertical turbulent velocity and the horizontal heat fluxes are determined by the equations:

$$<w^2> = \frac{1}{D}\left\{\frac{2}{3}E(1 + s_6 G_H) + \frac{4}{3}\alpha_3\alpha_6(\tau\beta g)^2 \times \right.$$
$$\left. \times <\theta^2>\left(1 - \frac{1}{2}\alpha_2\alpha_6 G_M + s_6 G_H\right)\right\}; \quad (11k)$$

$$<u\theta> = \frac{1}{D}\left\{\frac{2}{3}E\tau\frac{1}{\alpha_5}\left[\alpha_2 + (\alpha_2 + \alpha_6)s_6 G_H + \alpha_6\right]\tau\frac{\partial U}{\partial z}\right\}\frac{\partial \Theta}{\partial z} -$$
$$-\frac{1}{D}\tau\frac{\partial U}{\partial z}\alpha_6(\tau\beta g) <\theta^2> \{\alpha_6(1 + \frac{2}{3}\alpha_2^2 G_M) +$$
$$+(\alpha_6 - \frac{4}{3}\alpha_2)s_6 G_H + \frac{2}{3}s_6\alpha_2^2\alpha_3 G_M G_H - \frac{4}{3}s_6^2\alpha_2 G_H^2\}; \quad (11l)$$

$$<v\theta> = \frac{1}{D}\left\{\frac{2}{3}E\tau\frac{1}{\alpha_5}\left[\alpha_2 + (\alpha_2 + \alpha_6)s_6 G_H + \alpha_6\right]\tau\frac{\partial V}{\partial z}\right\}\frac{\partial \Theta}{\partial z} -$$
$$-\frac{1}{D}\tau\frac{\partial V}{\partial z}\alpha_6(\tau\beta g) <\theta^2> \{\alpha_6(1 + \frac{2}{3}\alpha_2^2 G_M) +$$
$$+(\alpha_6 - \frac{4}{3}\alpha_2)s_6 G_H + \frac{2}{3}s_6\alpha_2^2\alpha_3 G_M G_H - \frac{4}{3}s_6^2\alpha_2 G_H^2\}. \quad (11m)$$

1.3.3. Three-parameter model of stratified turbulence

To obtain closed equations for turbulent momentum and heat fluxes (11a)–(11m), it is needed to determine three parameters of turbulence: E, ε, and $<\theta^2>$.

In contrast to the traditional approach to modeling of the planetary boundary layer, when the parameterization of the form $\varepsilon \sim E^{3/2}/\Lambda$ (where Λ is the linear dimension of the energy-bearing turbulent eddies) is used for the KET dissipation rate, it seems preferable using another, more universal and common approach, in which ε is determined from the solution of the differential transfer equation (5a). Here this equation is used in the same form, as in Ref. 15, with the same numerical coefficients, whose values have been calibrated in the papers by different authors (see, for example, Refs. 11–14):

$$\sigma_E = 1.2, \quad \sigma_\varepsilon = 1.2, \quad \sigma_\theta = 0.6, \quad \psi_0 = 3.8,$$
$$\psi_1 = \psi_2 = 2.4, \quad \psi_3 = 0.3$$

(see Eqs. (12c)–(12e) below).

In the third-order closure turbulence model, all the three parameters of turbulence are determined from the closed differential transfer equations.

The differential transfer equation for destructions of temperature field pulsations is more difficult for calibration than the equation of KET dissipation. In place of this equation, simple parameterization of the relaxation form is used:

$$\varepsilon_\theta = <\theta^2>/\tau_\theta, \quad (12a)$$

where the temporal scale of the temperature field τ_θ is calculated through the ratio of the temporal scales of the temperature and dynamic fields:

$$R = \frac{\tau_\theta}{\tau} = \frac{<\theta^2>}{2\varepsilon_\theta}\frac{\varepsilon}{\tau}. \quad (12b)$$

The assumption that this parameter is constant gives the acceptable, in accuracy, results in both engineering[16] and geophysical flows[14] at $R \cong 0.6$.

For the diffusion terms D_{ii}, D_θ, and D_ε, simple approximations of gradient diffusion are accepted:

$$\frac{1}{2}D_{ii} = -\frac{\partial}{\partial x_i}\left(\frac{c_\mu}{\sigma_E}\frac{E^2}{\varepsilon}\frac{\partial E}{\partial x_i}\right), \quad (12c)$$

$$D_\varepsilon = -\frac{\partial}{\partial x_i}\left(\frac{c_\mu}{\sigma_\varepsilon}\frac{E^2}{\varepsilon}\frac{\partial \varepsilon}{\partial x_i}\right), \qquad (12d)$$

$$D_\theta = -\frac{\partial}{\partial x_i}\left(\frac{c_\mu}{\sigma_\theta}\frac{E^2}{\varepsilon}\frac{\partial <\theta^2>}{\partial x_i}\right). \qquad (12e)$$

Closed equations (2e), (4a), and (5a) form a three-parameter model of the thermally stratified turbulence.

1.4. Constants of the algebraic models for turbulent fluxes

Since the "standard" models,[8,9] used for the correlations of the dynamic field of turbulence with pressure pulsations, were successfully applied for the solution of various problems, the values of numerical coefficients in the model equations for these correlations have been tested quite well by now. They are presented in Ref. 9 as a graphical dependence of the form

$$(1 - c_2)/c_1 = 0.23. \qquad (12f)$$

For the "relaxation" coefficient in the model of the "slow" part $\Pi_{ij}^{(1)}$ of the pressure–velocity correlation (6b), it is taken that $c_1 = 2$ (from the usually used range from 1.5 to 2.0). For $c_1 = 2.0$, the coefficient c_2, determined from Eq. (12f), equals 0.54.

In selecting the value of the coefficient c_3 in the buoyancy terms ($c_3 B_{ij}$ in Eq. (6b)), it is possible to use the solution of simple problems with the allowance for the buoyancy effects[17,18] ($c_3 = 0.776$). Here, this coefficient is taken to be equal to 0.8, which corresponds to the value determined in Ref. 6 by the renorm-group method. The values of the coefficients in the pressure–temperature correlation Π_i^θ in Eq. (6b) are: $c_{1\theta} = 3.28$ and $c_{2\theta} = c_{3\theta} = 0.5$; they have been calibrated in modeling various turbulent stratified flows both uniform and nonuniform.[11,14] Note that the values of the coefficient c_1, calculated in Ref. 6 with the use of the renorm-group method, appeared to be 2.5.

At the same time, it should be kept in mind that, for example, for the widely used $k - \varepsilon$ model of turbulence, this method gives the values of the constants in the equation ε, which differ markedly from the values calibrated against measurements and usually used in calculations.

2. Numerical test

In the practice of modeling of environmental flows, a simple single-parameter K-theory with the isotropic turbulent viscosity coefficient (see, for example, Ref. 1) or the k–ε model (see, for example, Ref. 19), widely applied nowadays mostly due to the commercial software developed on the basis of the k–ε technology, is used.

Note that the above models of Reynolds shear stresses and the vector of the turbulent scalar flux provide for the additional possibilities of studying the effect of surface inhomogeneities (thermal and mechanical) on the structure of the stratified atmospheric flow as compared to the single- and two-parameter techniques of turbulence modeling. In particular, it becomes possible to study the effect of longitudinal turbulent heat diffusion on the main characteristics of the flow in the planetary boundary layer, such as, e.g., the layer height.

For the mesoscale turbulence model formulated, a simple two-dimensional numerical test was carried out. The atmospheric flow over the surface with the given roughness and a localized heat spot (model of an urban heat island) was modeled.

2.1. Computational procedure. Initial and boundary conditions

The horizontal dimension of the domain of integration is equal to 100 km with the 1-km resolution. The vertical resolution is 10 m within first 50 m from the surface with the following extension of the grid in the vertical direction up to a height of 1000 m. Higher, up to a height of 5000 m, the grid step was constant. The topography of the surface was plane with an urban island in the form of a heat spot (10 intervals in the horizontal direction) surrounded by rural areas.

The initial meteorological conditions were determined by the specified geostrophic wind (velocity of 3 and 5 m/s) in the eastward direction and the atmospheric thermal stratification, equal to 3.5 K/km for the potential temperature. The turbulent momentum and heat fluxes on the surface were calculated using Monin–Obukhov similarity theory for the near-surface layer.[20] The ground temperature was specified as

$$\Theta(x, 0, t) = 6\sin(\pi t/43200), \qquad (13)$$

where t is the current time, in s.

This is the only nonstationary boundary condition of the problem, which models the 24-hour cycle of solar heating of the Earth's surface. The heat island was defined as a temperature contrast with respect to the surface temperature by the same law (13), but with the amplitude increased by 2°. The normal derivatives of all the sought functions at the transverse boundaries were taken to be zero. The sought functions at the vertical boundary meet the same boundary condition.

The basic equations of the model [(1f), (1g), (1i), (2e), (4a), and (5a)] are solved by the method of alternating directions in combination with the sweep method on a shifted difference grid. The advective terms of the equations are approximated by the second scheme with the counter-flow differences.[21] The pressure distribution can be calculated simultaneously with the calculation of the velocity field from the diagnostic equation. However, in this study, applying the mesoscale model to the flow in ABL, we can assume that the vertical component of the wind velocity is much smaller than

the horizontal one. Thus, the hydrostatic approximation is assumed valid for the calculation of the pressure distribution. The vertical wind velocity is calculated as a quadrature from the continuity equation (1a), and its distribution is determined at the end of every computational cycle by integrating Eq. (1h) for the vertical velocity. The solution, independent of the computational grid, was obtained on a 120×50 grid. The time step is equal to 1.25 s of the real time.

2.2. Results of numerical simulation

2.2.1. Test for standard ABL

In the absence of a heat island, the formulated mesoscale model describes a 24-hour cycle of the ABL evolution with the given temperature distribution (13). The calculated distributions of the main characteristics agree with the observations and other calculations. As an example, Fig. 1 shows the distribution of the vertical heat flux. Curves *1–6* stand for the calculated profiles from 9:00 to 14:00. The calculated profiles are similar to the profiles of the vertical heat flux obtained using other numerical models.[23] The vertical heat flux profiles in Fig. 1 clearly demonstrate the effect of the entrainment processes. It can be seen that a wide zone between heights of 0.6 and $1.0z_i$ is affected by the entrainment processes, and the algebraic parameterization of turbulent fluxes of the third-order closure reproduces the alternation of the sign of the heat flux in the region of inversion as a response to cooling due to the entrainment process.

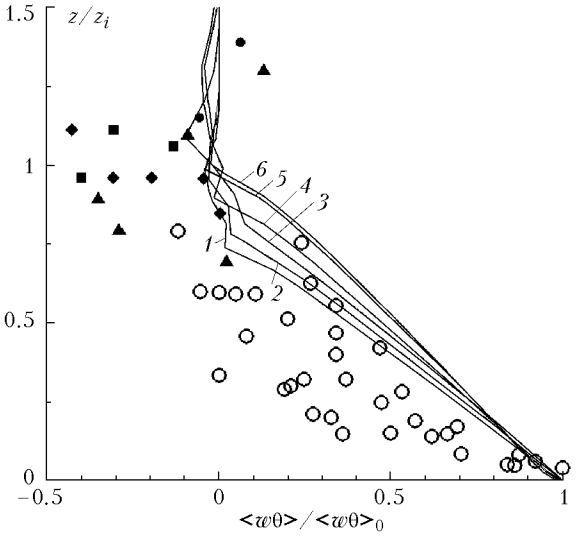

Fig. 1. Profiles of the turbulent vertical heat flux $\langle w\theta\rangle$, normalized to surface heat flux $\langle w\theta\rangle_0$: calculated (lines) and measured (symbols) in Ashchurch (closed symbols) and Minnesota (open symbols) [Ref. 22, Fig. 4.12].

2.2.2. Mesoscale flow over a heat island

This Subsection presents numerically calculated results on the mean wind and temperature distributions in comparison with the calculated data from Ref. 1, in which the effects of the urban surface were parameterized. In addition, since this third-order closure model of turbulent fluxes allows the effect of the longitudinal turbulent heat diffusion (first term in the right-hand side of Eq. (1i)) on the ABL characteristics to be followed, these results of the presented test are discussed as well.

Figure 2 shows the vector field of the mean horizontal wind and isotachs of the vertical component of the mean wind for 12:00 a.m. of the diurnal cycle of modeling for the geostrophic wind velocity equal to 3 and 5 m/s, respectively. The isotachs clearly demonstrate the upward flows at the boundaries of the heat island, where there is a sharp temperature contrast between the heat island and its environment.

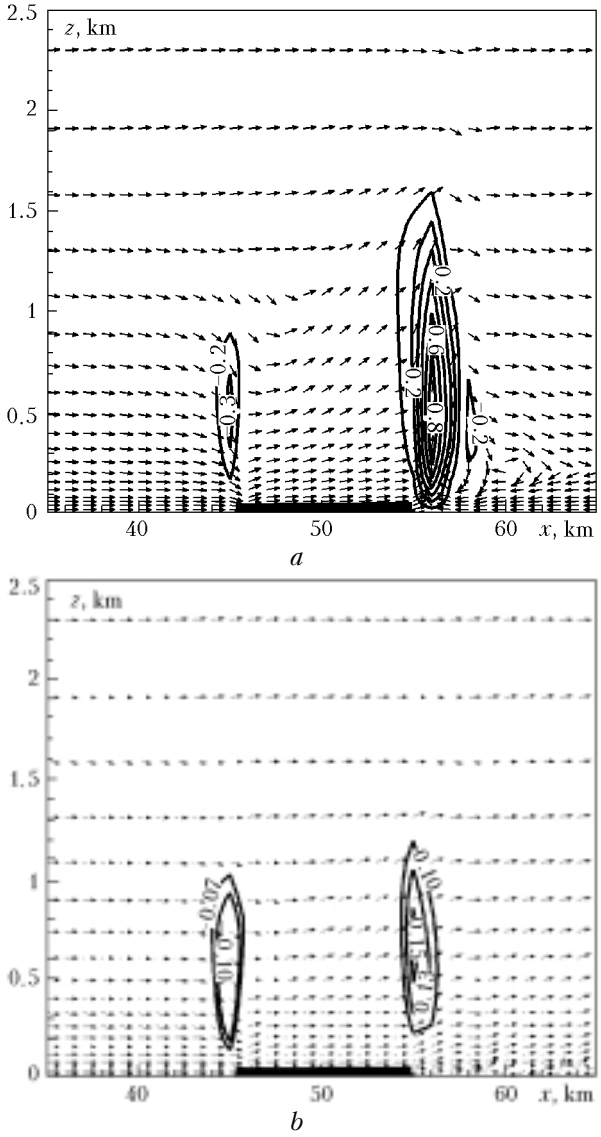

Fig. 2. Vector field and isotachs of the mean horizontal wind at 15:00 in the diurnal cycle of modeling for the geostrophic wind velocity $U_G = 3$ (*a*) and 5 m/s (*b*).

Figures 3*a* and *b* depict the vertical sections of the deviations of the potential temperature (*a*) and the mean wind field (*b*) calculated in Ref. 1 for 12:00 a.m. in the diurnal cycle of modeling. These calculations employed a single-parameter model of turbulence (all turbulent momenta and heat fluxes are determined by the gradient Boussinesq model with the turbulent viscosity coefficient) and parameterization of the main factors of the heterogeneous urban surface (head resistance of buildings, radiative processes in city canyons). Figures 3*c* and *d* show the same sections over the modeled heat island obtained with the mesoscale model, described in this paper, with the neglected morphology of the urban surface. In both of the cases, the same test for the 2D area (see Subsection 2.1 above) and the same initial distribution of the potential temperature and the geostrophic wind were used.

The results of both tests cannot be compared quantitatively because of different parameterization of the effect of the urban heat island and the effects of the urban roughness, which significantly change the structure of the flow directly in the layer of obstacles, a part of the urban atmospheric boundary layer adjacent to the surface. However, the large-scale air circulation within the domain of integration in both of the numerical tests can be compared qualitatively.

It should be noted, in addition, that the verification of one or another parameterization of the turbulent exchange processes within urban surfaces always present severe difficulties either due to the absence of field measurements or due to the heterogeneity of urban surfaces, which is always very high. The vertical sections of the field of the potential temperature are similar.

In Figs. 3*a* and *c*, the dash-and-dot and the dashed lines show the height of the boundary layer, determined by the lowest level of the model, at which KET is lower than 0.01 m^2/s^2. It can be seen that above the city there is a column of heated, unstable air, which is shifted by the advection in the windward direction.

The effect of the urban surface on the height of the boundary layer is more obvious in modeling with

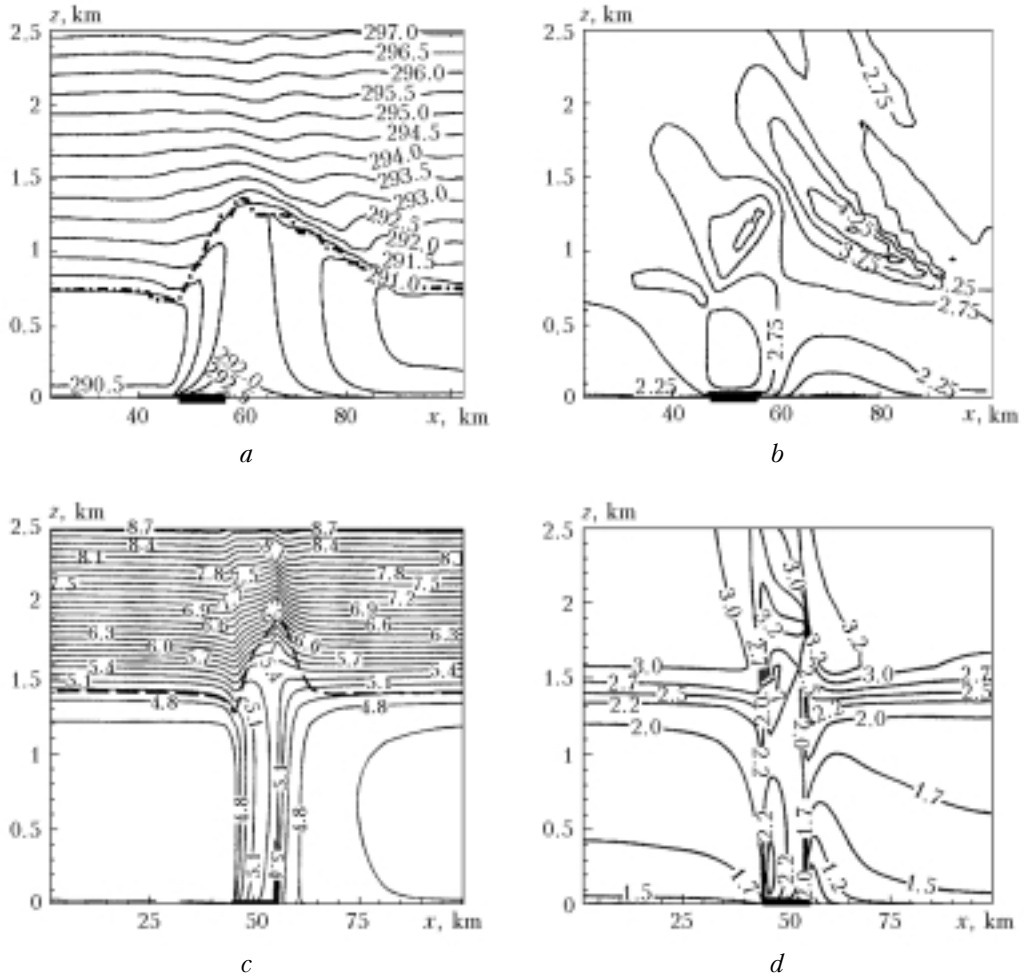

Fig. 3. Vertical sections of the fields of the potential temperature (*c*) and the mean horizontal wind (*d*) at 12:00 a.m. as calculated in Ref. 1 (*a*, *b*) and in this work (*c*, *d*) (U_G = 3 m/s).

parameterization of the morphology of the urban surface due to the effect of the urban roughness.

The wind velocity (Figs. 3*b* and *d*) increases over the city and the heat spot, because the vertical temperature gradient between the air above the city (heat spot) and the air above the city surroundings generates the thermal circulation, which can be seen from the isotachs of the vertical velocity in Fig. 2. In addition, the pressure gradient, caused by higher temperatures over the city (heat spot), has here the same sign as the advection. Along with the effects of friction near the surface, this leads to the lower wind values near the urban surface and higher values above it. The minimum in the wind velocity downstream out of the city (heat spot) arises because the pressure gradient and the advection of the synoptic wind have the opposite signs in this area. The presence of such a "cap" of the warm air above the urban heat island was observed, in particular, in laboratory measurements[24] and in numerical investigations.[14,15]

Figure 4 shows the calculated vertical sections of the deviations of the potential temperature and the mean horizontal wind in modeling at the geostrophic wind velocity $U_G = 5$ m/s. The comparison of Fig. 3*c* and Fig. 4*a* indicates the decrease in the height of the boundary layer with the increase of the wind velocity. The same result was also obtained in the test carried out in Ref. 1.

The calculated results shown in Fig. 5 allow estimating the effect of the longitudinal turbulent heat diffusion, determined by the first term in the right-hand side of Eq. (1i), on the boundary layer characteristics. It is seen from Fig. 5 that the height of the boundary layer (marked by the dashed line) in the presence of diffusion is higher than in its absence. The longitudinal diffusion transports the heat into the column of the heated air above the city (heat spot), which increases the KET generation due to the fluctuating buoyancy force and favors the increase of the PBL height.

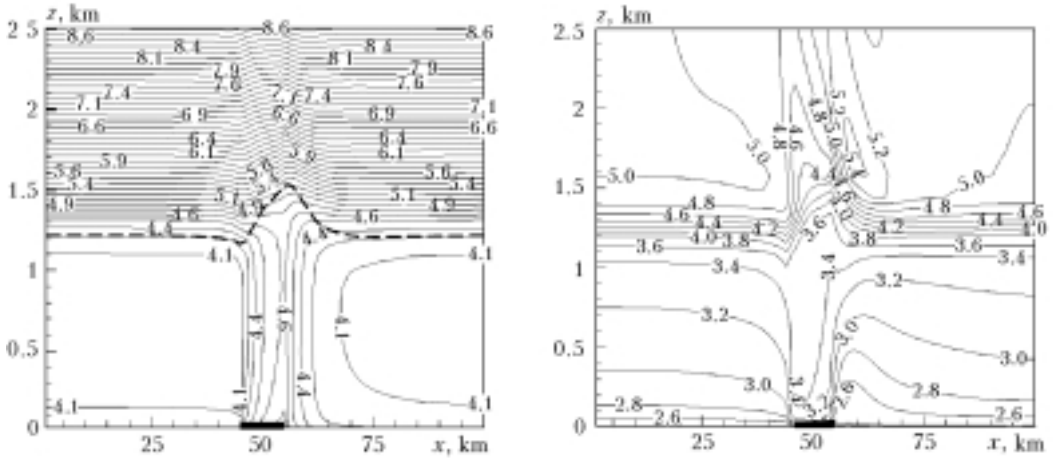

Fig. 4. Calculated vertical sections of the deviations of the potential temperature (*a*) and the mean horizontal wind (*b*) at 12:00 a.m. ($U_G = 5$ m/s).

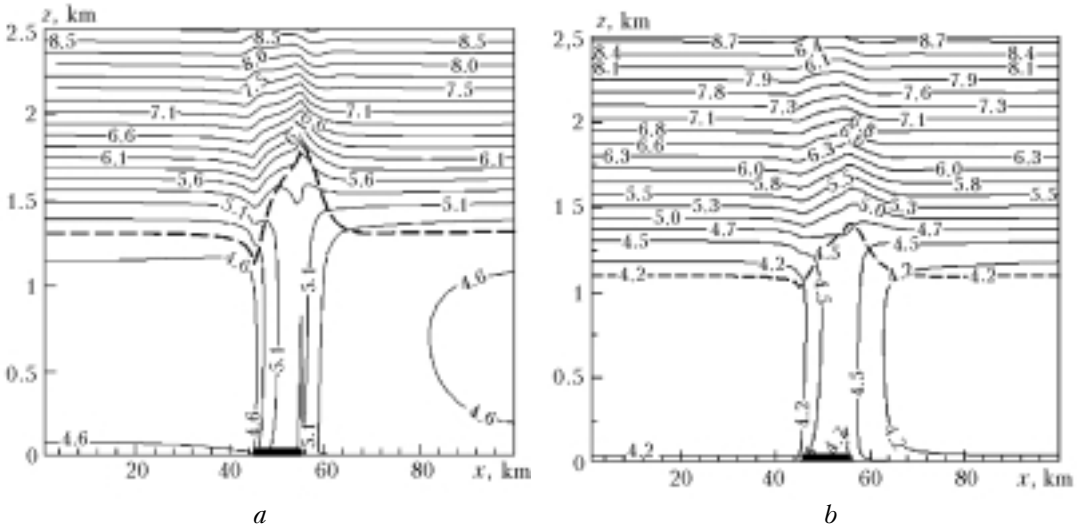

Fig. 5. Vertical sections of the deviations of the potential temperature, calculated taking into account (*a*) and neglecting (*b*) the longitudinal turbulent heat diffusion at 12:00 a.m. ($U_G = 5$ m/s).

Conclusions

In this paper, we have presented the three-parameter model of anisotropic turbulent momentum and heat fluxes for modeling of atmospheric mesoscale flows over a thermally nonuniform surface. A simple two-dimensional numerical test of the effect of the heat spot on the Earth's surface, simulating the urban heat island, on the structure of the atmospheric boundary layer has been performed.

The computer simulations are in a qualitative agreement with the results of analogous tests, carried out with the mesoscale model, which employs the single-parameter model of turbulence with a carefully selected linear scale of turbulence and accounts for both the thermal and mechanical effects of the urban surface on the boundary layer structure.

The formulated third-order closure model of turbulent fluxes allows the effects of turbulent transfer to be studied under conditions of both thermal and mechanical heterogeneity of the surface. In particular, it is shown that the longitudinal turbulent heat diffusion favors the increase of the boundary layer thickness. The single- and two-parameter models of the atmospheric boundary layer usually neglect the effects of the longitudinal turbulent transfer.

Acknowledgments

This work was supported, in part, by the Russian Foundation for Basic Research (Grants No. 03–05–64005 and No. 04–05–64562), the Integration Project of the Presidium of SB RAS (Grant No. 130), and the Program "Universities of Russia" (Grant No. 01.01.190).

References

1. A. Martilli, J. Appl. Meteorol. **41**, No. 12, 1247–1266 (2002).
2. M. Roth, Quart. J. Roy. Meteorol. Soc. **126**, 941–990 (2000).
3. G.L. Mellor and T. Yamada, J. Atmos. Sci. **31**, No. 10, 1791–1806 (1974).
4. G.L. Mellor and T. Yamada, Rev. Geophys. and Space Phys. **20**, No. 4, 851–875 (1982).
5. A.N. Kolmogorov, Izv. Akad. Nauk SSSR, Ser. Fiz. **6**, Nos. 1–2, 56–58 (1942).
6. Y. Cheng, V.M. Canuto, and A.M. Howard, J. Atmos. Sci. **59**, 1550–1565 (2002).
7. O. Zeman and J.L. Lumley, in: *Turbulent Shear Flows*, Vol. 1, ed. by F. Durst et al. (Springer-Verlag, 1979), pp. 295–302.
8. B.E. Launder, G. Reece, and W. Rodi, J. Fluid Mech. **68**, 537–566 (1975).
9. B.E. Launder, in: *Simulation and Modeling of Turbulent Flows*, ed. by T.D. Gatski et al. (Oxford University Press, New York, 1996), pp. 243–302.
10. S.S. Girimaji and S. Balachandar, Int. J. Heat and Mass Transfer **41**, Nos. 6–7, 915–929 (1998).
11. T.P. Sommer and R.M.C. So, Phys. Fluids **7**, No. 11, 2766–2777 (1995).
12. A. Andren, J. Appl. Meteorol. **29**, No. 3, 224–239 (1990).
13. A. Andren, Boundary-Layer Meteorol. **56**, 207–221 (1990).
14. A.F. Kurbatskii, J. Appl. Meteorol. **40**, No. 10, 1748–1761 (2001).
15. A.F. Kurbatskii and L.I. Kurbatskaya, Izv. Ros. Akad. Nauk, Fiz. Atmos. Okeana **37**, No. 2, 149–161 (2001).
16. A.F. Kurbatskii and F.V. Kazakov, Thermophys. and Aeromechanics **6**, No. 2, 231–240 (1999).
17. M.M. Gibson and B.E. Launder, J. Fluid Mech. **86**, No. 3, 491–511 (1978).
18. J.L. Lumley and P. Monsfield, Boundary-Layer Meteorol. **30**, 109–142 (1984).
19. T.C. Vu, Y. Ashie, and T. Asaeda, Boundary-Layer Meteorol. **102**, 459–490 (2002).
20. J.F. Louis, Boundary-Layer Meteorol. **17**, No. 2, 187–202 (1979).
21. P.J. Roache, *Computational Fluid Dynamics* (Albuquerque, 1976).
22. S.J. Caughey, "*Experimental data on the atmospheric boundary layer*," in: *Atmospheric Turbulence and Air Pollution Modelling*, ed. by F.T.M Nieuwstadt and H. van Dop (Reidel, Dordrecht, 1982).
23. J.C. Andre, G. De Moor, P. Lacarrere, G. Therry, and R. du Vachat, J. Atmos. Sci. **35**, No. 10, 1861–1883 (1978).
24. J. Lu, S.P. Arya, W.H. Snyder, and R.E. Lawson, Jr., J. Appl. Meteorol. **36**, No. 10, 1377–1402 (1997).